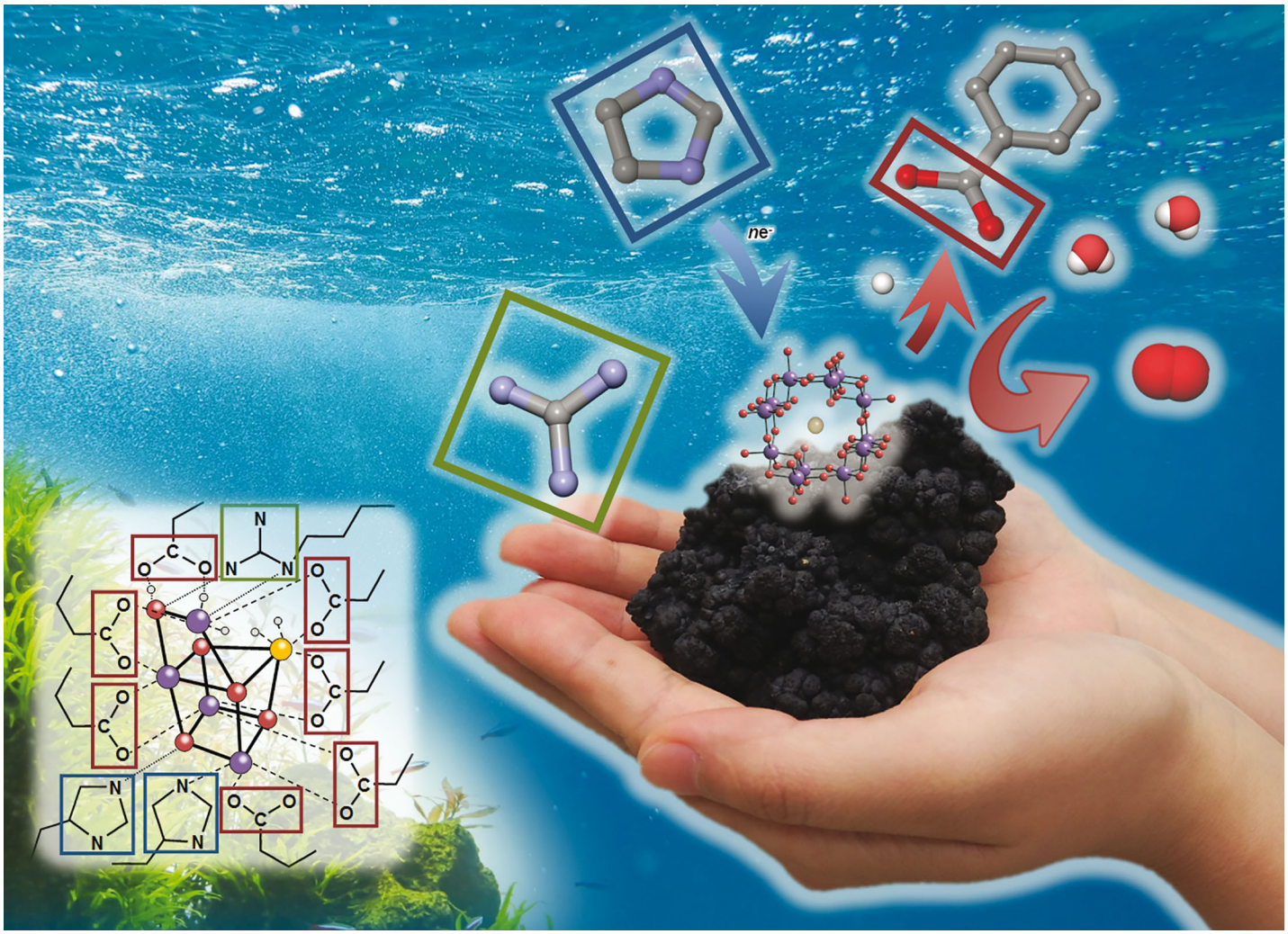


**Showcasing research from the group of Dr Ryuhei Nakamura at RIKEN Center for Sustainable Resource Science (CSRS), Japan.**

Stability of organic compounds on the oxygen-evolving center of photosystem II and manganese oxide water oxidation catalysts

The organic residues surrounding the $Mn_4$ cluster in photosystem II are known to be indispensable for their high water oxidation activity. Here, carboxyl groups, which are the most abundant residues around the $Mn_4$ cluster, were found to stably facilitate electrochemical water oxidation by manganese oxides.

## As featured in:


See Ryuhei Nakamura *et al.*, *Chem. Commun.*, 2016, **52**, 13760.

ROYAL SOCIETY OF CHEMISTRY

www.rsc.org/chemcomm

Registered charity number: 207890

ChemComm

COMMUNICATION

View Article Online
View Journal | View Issue



Cite this: *Chem. Commun.*, 2016, 52, 13760

Received 30th August 2016,
Accepted 25th October 2016

DOI: 10.1039/c6cc07092b

www.rsc.org/chemcomm

# Stability of organic compounds on the oxygen-evolving center of photosystem II and manganese oxide water oxidation catalysts†

Toru Hayashi,[a] Akira Yamaguchi,[b] Kazuhito Hashimoto[c] and Ryuhei Nakamura*[b]

**Surrounding organic residues are indispensable for the high water oxidation activity of the $Mn_4$ cluster in photosystem II. Here, the stability of organic compounds on synthetic Mn oxides was analyzed using inlet electrochemical mass spectroscopy. Carboxyl groups, which are the most abundant residues around the $Mn_4$ cluster, were found to stably facilitate the oxygen evolution reaction.**

Efficient and stable non-noble-metal-based catalysts for the oxygen evolution reaction (OER) *via* water oxidation ($2H_2O \rightarrow O_2 + 4H^+ + 4e^-$) are highly desirable for the generation of electrons needed to reduce protons or $CO_2$ to produce chemical fuels.[1] In nature, the $Mn_4$ cluster ($CaMn_4O_5$) of photosystem II (PSII) catalyzes the OER[2] with an overpotential of approximately 300 mV[1b,3] and a maximum turnover frequency of $\sim 10^3$ $s^{-1}$.[2d] Nine amino-acid residues belonging to the two proteins (D1 and CP43) of PSII are directly coordinated or hydrogen-bonded to the cluster (Fig. 1a) and provide a structural and electrostatic environment that is indispensable for the function and stability of PSII.[2a] The importance of these amino acids is demonstrated by the fact that any point mutation of the nine residues drastically reduces the activity of the $Mn_4$ cluster for the OER.[4] D1-Asp61 has also been regarded as an important residue as a proton acceptor in the concerted proton–electron transfer (CPET) to prevent the charge buildup during the Kok cycle and the starting point of the proton exit pathway,[5] which is also shown in Fig. 1a. The residues, however, seem to be at risk for the oxidative decomposition, because the chlorophyll dimer $P_{680}$ in PSII generates the highest oxidative potential known in biology (1.15–1.26 V *vs.* SHE)[6] for initiating the OER. In fact, it remains uncertain whether the histidine directly liganded to the $Mn_4$ cluster, D1-His332 (Fig. 1a), is subject to one-electron oxidation to a transient radical during the Kok cycle.[2c,7] Still, the residues around the $Mn_4$ cluster are highly stable against oxidative decomposition and therefore the turnover number of PSII can reach as high as $\sim 10^6$,[2e] even if transient oxidation is operative in this system.

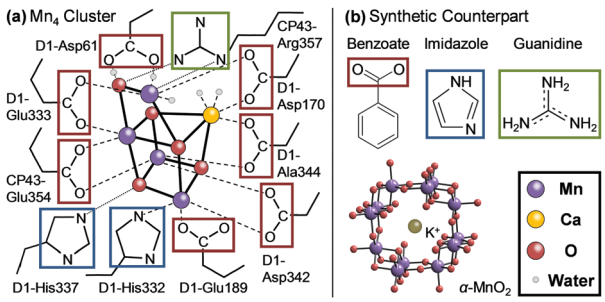


Fig. 1 (a) A schematic diagram of the ligand environment around the $Mn_4$ cluster in PSII adapted from ref. 2*a* (broken lines: coordination bonds, dotted lines: hydrogen bonds). (b) The synthetic counterpart of PSII examined in this study. The red, blue, and green boxes are shown around carboxyl, imidazolyl, and guanidino groups, respectively.

Recently, several beneficial roles of organic compounds on Mn-based catalysts for the OER at neutral pH were revealed. For example, the coordination of nitrogen-containing organic ligands to the octahedral Mn site of Mn oxides enhances the OER activity,[8] a response that is attributed to the increased stabilization of $Mn^{3+}$, a reaction intermediate of the OER.[9] The improved stability of $Mn^{3+}$ is ascribed to the asymmetric ligand field, where the two $e_g$ orbitals of $Mn^{3+}$ have different energies and therefore the charge disproportionation of $Mn^{3+}$ to $Mn^{2+}$ and $Mn^{4+}$ for eliminating the orbital degeneracy is effectively suppressed.[8,10] In addition, pyridine derivatives were shown to enhance the OER activity of Mn oxides by inducing CPET, thereby reducing the required potential for the generation of $Mn^{3+}$ *via* electrochemical oxidation of $Mn^{2+}$.[11] The enhanced OER activity of Mn oxides modified by amino-acid residues or other ligands was also reported by Najafpour *et al.*[12] The selection

[a] *Department of Applied Chemistry, The University of Tokyo, 7-3-1 Hongo, Bunkyo-ku, Tokyo 113-8656, Japan*
[b] *Biofunctional Catalyst Research Team, RIKEN Center for Sustainable Resource Science (CSRS), 2-1 Hirosawa, Wako, Saitama 351-0198, Japan. E-mail: ryuhei.nakamura@riken.jp*
[c] *National Institute for Materials Science (NIMS), 1-2-1 Sengen, Tsukuba, Ibaraki 305-0047, Japan*

† Electronic supplementary information (ESI) available: Detailed experimental conditions, supplementary figures and discussion. See DOI: 10.1039/c6cc07092b

of ligands is also of particular importance for the construction of molecular catalysts for the OER.[1f] However, the synthetic systems described above generally undergo self-oxidation and result in the degradation of organic compounds.

Although organic compounds are indispensable for the efficient OER for both natural and artificial Mn-based catalysts, there is a distinct difference in the stability against the self-oxidation. As determining the origin of the different stability is expected to provide a new design strategy of Mn-based OER catalysts that are highly efficient and stable under neutral conditions, here we analyzed the possible oxidation pathways of organic compounds in a synthetic counterpart and compared them with extant PSII from the viewpoint of energetics.

Russell, Hall, Sauer, and Yachandra proposed that the $Mn_4$ cluster in PSII originated from a Mn mineral.[13] Sauer and Yachandra further speculated based on the bond length that the origin was a tunnel-type Mn oxide, such as α-$MnO_2$ with all four Mn cluster arrangements possible in this mineral class (Fig. 1b).[13b] Fine-tuning of the catalytic activity was also proposed to occur through the reorganization and modification of the Mn oxide mineral during its incorporation into a protein.[13b] Regardless of the underlying process, the interaction between a complexed Mn compound and the surrounding amino-acid residues would have influenced the evolution of the catalytic ancestor of PSII. In the present study, α-$MnO_2$ and several artificial amino-acid analogs, including benzoate, imidazole, and guanidine, were therefore used as a synthetic model of the reaction center of PSII (Fig. 1b).

Anodic reactions by α-$MnO_2$ electrodes in an electrolyte containing artificial amino-acid analogs were first investigated by measuring the anodic current and the evolution of $O_2$ and $CO_2$ over a range of potentials using a potentiostat, needle-type $O_2$ microsensor, and inlet electrochemical mass spectroscopy (EC-MS) system. Particulate film electrodes were prepared with the synthesized α-$MnO_2$ powder[14] using a spray deposition method, as previously described.[11] The artificial amino-acid analogs benzoate, imidazole, and guanidine were dissolved in the electrolyte, which consisted of 0.5 M $Na_2SO_4$. The pH of the electrolyte was adjusted using NaOH and $H_2SO_4$. Detailed experimental conditions are described in the ESI.†

The presence of benzoate in the electrolyte increased both the anodic current and concentration of dissolved $O_2$ generated by the α-$MnO_2$ electrode (Fig. 2a). In the absence of benzoate, the slope of the Tafel plot was 120.7 mV (Fig. 2a-1, inset), indicating that the rate-determining step (RDS) of the OER is a one-electron transfer reaction.[15] In addition, the potential at a constant current was not dependent on the pH (Fig. S1, ESI†), indicating that the reaction order of the proton concentration in the total reaction rate was zero. This further suggested that proton transfer was not involved in the RDS or during the pre-equilibrium phase of the step.[15] The results from the mechanistic analysis are consistent with previous reports that the RDS of the OER on α-$MnO_2$ is the one-electron oxidation from $Mn^{2+}$ to $Mn^{3+}$ without proton transfer.[9,11] In contrast, after the addition of benzoate to the electrolyte, the slope value of the Tafel plot decreased (Fig. 2a-1, inset) and the potential at a

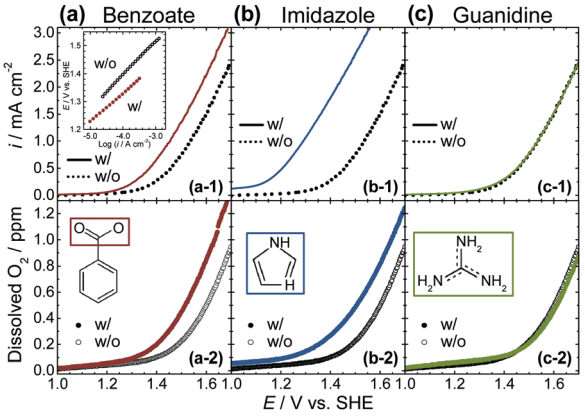


Fig. 2 Changes in anodic current density and dissolved $O_2$ concentration for α-$MnO_2$ electrodes by the addition of artificial amino-acid analogs (pH 7.5, scan rate: 1 mV $s^{-1}$, concentration of benzoate, imidazole (deprotonated form), and guanidine: 50 mM). Inset: Tafel plots (slope: 101.4 mV $dec^{-1}$ (w/benzoate), 120.7 mV $dec^{-1}$ (w/o)).

constant current exhibited pH dependence (Fig. S1, ESI†). The H/D kinetic isotope effect also increased from 1.18 ± 0.09 to 1.45 ± 0.05 (pH(pD) 7; other experimental details are given in the ESI†). These results affirm that the reaction order of the proton concentration increased in the total reaction rate equation by the addition of benzoate.[15] The observed enhancement of the OER activity in response to the induction of proton transfer is consistent with our previous finding that CPET is required to avoid the formation of high-energy intermediates ($Mn^{3+}$–$OH_2$), leading to the enhancement of the activity for the OER.[11] Considering the libido rule of general acid–base catalysis,[16] which states that the p$K_a$ values of bases have to be intermediate between the p$K_a$ value of $Mn^{3+}$–$OH_2$ (0.7) and that of $Mn^{2+}$–$OH_2$ (10.6) to induce CPET,[11,16] benzoate is eligible to be a CPET inducer, as the p$K_a$ value is 4.2.[17] Further, FT-IR measurement showed the formation of an outer-sphere complex of benzoate and the surface of α-$MnO_2$, a suitable configuration for the induction of CPET (Fig. S2 and S3, ESI†).

The effect of imidazole on the OER was also examined (Fig. 2b). In the presence of imidazole, a 250 mV negative shift in the onset potential of the anodic current ($E_{onset}$), defined as the potential at a current density of 0.5 mA $cm^{-2}$, was observed for the α-$MnO_2$ electrode (Fig. 2b-1). However, the magnitude of the onset potential shift of the $O_2$ production monitored by the $O_2$ microsensor was only 130 mV (at 0.2 ppm), which was substantially smaller than the shift in $E_{onset}$ (Fig. 2b-2). The shift in the onset potential of the $O_2$ production was also smaller than that of $E_{onset}$ when histidine was added to the electrolyte (Fig. S4, ESI†). The large difference in the potential shift for the onset of anodic current and $O_2$ production implied that the oxidation of imidazole and histidine proceeded in a more negative potential region than that for the OER.

To further examine the reason for this difference, *in situ* EC-MS for the simultaneous monitoring of the anodic current and mass signals of volatile products, and UV-vis measurements were conducted. During an anodic potential scan of α-$MnO_2$ in the presence of imidazole, increases in the ion current for $O_2$

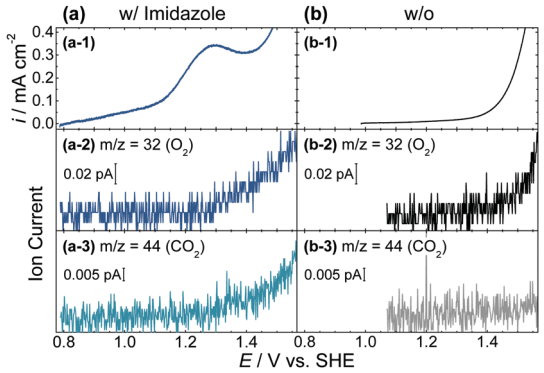


Fig. 3 (a-1 and b-1) Current density and (a-2, 3 and b-2, 3) mass signals during the anodic potential scan of α-$MnO_2$ electrodes before and after the addition of 50 mM of the deprotonated form of imidazole (pH 7.5, scan rate: 0.5 mV $s^{-1}$, unstirred).

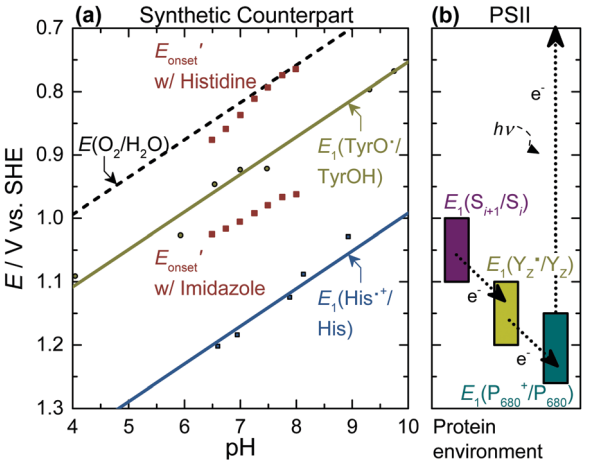


Fig. 4 Thermodynamic potential values related to the oxidation of imidazole and histidine (a) on α-$MnO_2$ and (b) around the $Mn_4$ cluster. The presented values included those experimentally obtained in this study and reported in the literature.[2d,3,6,18–20] (Potential *vs.* SHE was calculated using the reported potential of SHE *vs.* vacuum, +4.28 V.[21])

($m/z$ = 32) were detected with simultaneous production of $CO_2$ ($m/z$ = 44) at the onset potential of approximately 1.25 V (*vs.* SHE) (Fig. 3a-2 and a-3). No other volatile products, such as NO and $NO_2$, were detected in the EC-MS analysis. However, the onset potential of the anodic current was approximately 0.8 V, which was 250 mV more negative than that of the ion current for $O_2$ (Fig. 2b and 3a). These results demonstrated that the Coulombic efficiency for the OER between 0.8 and 1.25 V was determined to be zero. In the absence of imidazole, the ion current for $O_2$ accompanied by the anodic current and $CO_2$ was not detected (Fig. 3b). Furthermore, a decrease in the time-dependent *in situ* UV-vis absorption of α-$MnO_2$ electrodes in contact with the electrolyte supplemented with imidazole at resting potential, centered at 510 nm, was observed (Fig. S5, ESI†), with new FT-IR peaks assignable to the oxidation products of imidazole (Fig. S6, ESI†), indicating that electrons injected from imidazole to α-$MnO_2$ were used to reduce $Mn^{4+}$ to form soluble $Mn^{2+}$ ions. These results are consistent with the expectation that, although imidazole enhanced OER, the oxidation of imidazole proceeded in a more negative potential region than that for the OER with the concurrent dissolution of $Mn^{2+}$.

In contrast to benzoate and imidazole, the addition of guanidine to the electrolyte resulted in a negligible difference in both the anodic current and OER (Fig. 2c). This finding is consistent with the fact that the p$K_a$ value of guanidine is 13.6,[17] which exceeds the maximum permissible value to function as a CPET inducer. It also showed that the oxidation of guanidine was negligible in the potential range for the measurement.

The electrochemical analysis of the function of amino-acid analogs using the synthetic counterpart of PSII revealed that benzoate enhanced the OER activity by inducing CPET (Fig. 2a and Fig. S1, ESI†). Although imidazole also enhanced the OER activity, oxidation of imidazole and dissolution of α-$MnO_2$ severely competed with the OER (Fig. 2b and 3), a property that is in sharp contrast with the stable existence of the histidine ligands, D1-His332, and the catalytic core of the $Mn_4$ cluster in PSII (Fig. 1a).

To better understand the reasons for the stability differences of the systems composed of imidazolyl group and α-$MnO_2$ or the $Mn_4$ cluster, we constructed pH-dependent energy diagrams of water and amino acid oxidation for these systems (Fig. 4). The constructed diagrams include the equilibrium potential of the OER, the potential of the α-$MnO_2$ electrodes at 10 μA $cm^{-2}$ ($E_{onset}'$) in the presence of imidazole or histidine measured in the present study, the redox potential of the one-electron oxidation ($E_1$) of histidine in aqueous solution determined in a previous pulse radiolysis study,[18] and the reported $E_1$ values of tyrosine in aqueous solution,[19] $Mn_4$ cluster ($E_1(S_{i+1}/S_i)$),[2d,3] redox-active tyrosine residue D1-Tyr161 ($Y_Z$),[2d,3,20] and $P_{680}$[6] in PSII. To our knowledge, the experimental $E_1$ value of imidazole has not been reported to date. However, this value can be estimated from the reported experimental value of vertical ionization energy (VIE).[22] Details of this calculation are provided in the ESI.†

Based on the pH-dependent energy diagram, it was found that $E_1$ of histidine is approximately 300 mV more positive than $E_{onset}'$ in the presence of histidine (Fig. 4a) at pH values ranging from 6 to 8. $E_1$ of imidazole was also estimated to be more positive than $E_{onset}'$ in the presence of imidazole (ESI†), suggesting that the one-electron oxidation reaction of histidine and imidazole is thermodynamically unfavorable on α-$MnO_2$ at neutral pH. As $E_{onset}'$ in the presence of histidine and imidazole showed pH dependence, it appears that the experimentally observed decomposition of histidine and imidazole on α-$MnO_2$ (Fig. 2b, 3 and Fig. S4, ESI†) is a consequence of a proton-coupled multi-electron oxidation reaction, which results in the simultaneous dissolution of $Mn^{2+}$ (Fig. S5, ESI†).

Then, how is the oxidation of imidazolyl groups effectively prevented in PSII? In PSII, a potential cascade exists between $P_{680}$ and the $Mn_4$ cluster, with $Y_Z$ serving as an intermediate (Fig. 4b). In addition, the $E_1$ values of aromatic amino acids such as tryptophan and tyrosine are predicted to be more positive in protein environments compared to aqueous solutions because of the low dielectric constant of the former (~3–5 in PSII)[2g] and the lack of effective protonic contact with the bulk

 

solution which allows deprotonation.[20,23] Consistent with this prediction, the $E_1$ value of $Y_Z$ was found to be approximately 100–200 mV more positive than that of tyrosine in aqueous solution, as shown in Fig. 4a. If the same mechanism holds true for the $E_1$ value of imidazolyl groups in protein environments, the generation of transient histidine radicals *via* the one-electron oxidation of D1-His332 (Fig. 1a) may also be thermodynamically unfavorable.

The present study also revealed that benzoate functions as an efficient and stable activator of the OER catalyzed by α-$MnO_2$ at neutral pH (Fig. 2a). In PSII, six of the seven direct ligands of the $Mn_4$ cluster are carboxyl groups (Fig. 1a).[2a] Also, the carboxyl group of D1-Asp61 has been considered to act as a proton acceptor in the CPET in the Kok cycle.[5] This exclusive utilization of carboxyl groups is a distinct feature of this enzyme from others. For example, the oxygen reduction reaction (ORR), which is the reverse reaction of the OER, is catalyzed by Cu and Fe coordinated by thiol, imidazolyl groups, or porphyrin nitrogen, but not by carboxyl groups.[24] Therefore, it appears that, in the course of evolution, the carboxyl residues were adapted by PSII because of their high durability against self-oxidation during the OER. The introduction of carboxyl groups represents an intriguing strategy to develop stable Mn-based OER catalysts that are highly active under neutral conditions.

In summary, we analyzed the effects and the stability of the organic compounds in a synthetic counterpart of PSII. The comparison of energy diagram of the OER catalyzed by PSII and the synthetic counterpart suggested that imidazolyl groups are oxidized at the surface of α-$MnO_2$ to generate soluble $Mn^{2+}$ ions *via* a proton-coupled multi-electron oxidation pathway, while both single and multi-electron oxidation reactions of D1-His332 are effectively inhibited in PSII. In addition, the presence of carboxyl groups, which are abundant around the $Mn_4$ cluster,[2a] was found to stably facilitate the OER activity of α-$MnO_2$ by inducing the CPET reaction. These findings are expected to provide a new design rationale of organic ligands, which is crucial for the development of functional analogues of the $Mn_4$ cluster for efficient and stable water splitting at neutral pH.

We thank Dr K. Kamiya (Osaka Univ.) for providing access to the EC-MS equipment and K. Jin (Seoul Natl. Univ.) for advice on measuring Tafel plots. This work was supported by JSPS Grant-in-Aid for Scientific Research no. 26288092. T. H. acknowledges Grant-in-Aid for JSPS Fellows no. 15J10583.

## Notes and references

1 (*a*) A. Fujishima and K. Honda, *Nature*, 1972, **238**, 37; (*b*) H. Dau, C. Limberg, T. Reier, M. Risch, S. Roggan and P. Strasser, *ChemCatChem*, 2010, **2**, 724; (*c*) Y. Zhao, R. Nakamura, K. Kamiya, S. Nakanishi and K. Hashimoto, *Nat. Commun.*, 2013, **4**, 2390; (*d*) F. Jiao and H. Frei, *Chem. Commun.*, 2010, **46**, 2920; (*e*) K. Jin, A. Chu, J. Park, D. Jeong, S. E. Jerng, U. Sim, H.-Y. Jeong, C. W. Lee, Y.-S. Park, K. D. Yang, G. K. Pradhan, D. Kim, N.-E. Sung, S. H. Kim and K. T. Nam, *Sci. Rep.*, 2015, **5**, 10279; (*f*) M. D. Kärkäs, O. Verho, E. V. Johnston and B. Åkermark, *Chem. Rev.*, 2014, **114**, 11863.

2 (*a*) Y. Umena, K. Kawakami, J.-R. Shen and N. Kamiya, *Nature*, 2011, **472**, 55; (*b*) M. Suga, F. Akita, K. Hirata, G. Ueno, H. Murakami, Y. Nakajima, T. Shimizu, K. Yamashita, M. Yamamoto, H. Ago and J.-R. Shen, *Nature*, 2015, **517**, 99; (*c*) J. Yano and V. Yachandra, *Chem. Rev.*, 2014, **114**, 4175; (*d*) D. J. Vinyard, M. Gennady, G. M. Ananyev and G. C. Dismukes, *Annu. Rev. Biochem.*, 2013, **82**, 577; (*e*) N. Cox, M. Retegan, F. Neese, D. A. Pantazis, A. Boussac and W. Lubitz, *Science*, 2014, **345**, 804; (*f*) K. Ogata, T. Yuki, M. Hatakeyama, W. Uchida and S. Nakamura, *J. Am. Chem. Soc.*, 2013, **135**, 15670; (*g*) P. E. M. Siegbahn, *Biochim. Biophys. Acta*, 2013, **1827**, 1003.

3 H. Dau and I. Zaharieva, *Acc. Chem. Res.*, 2009, **42**, 1861.

4 (*a*) P. J. Nixon and B. A. Diner, *Biochemistry*, 1992, **31**, 942; (*b*) R. J. Debus, K. A. Campbell, D. P. Pham, A. M. A. Hays and R. D. Britt, *Biochemistry*, 2000, **39**, 6275; (*c*) H. A. Chu, A. P. Nguyen and R. J. Debus, *Biochemistry*, 1995, **34**, 5859; (*d*) H. J. Hwang, P. Dilbeck, R. J. Debus and R. L. Burnap, *Biochemistry*, 2007, **46**, 11987.

5 T. J. Meyer, M. H. V. Huynh and H. H. Thorp, *Angew. Chem., Int. Ed.*, 2007, **46**, 5284.

6 (*a*) F. Rappaport, M. Guergova-Kuras, P. J. Nixon, B. A. Diner and J. Lavergne, *Biochemistry*, 2002, **41**, 8518; (*b*) M. Grabolle and H. Dau, *Biochim. Biophys. Acta, Bioenerg.*, 2005, **1708**, 209; (*c*) T. Shibamoto, Y. Kato, M. Sugiura and T. Watanabe, *Biochemistry*, 2009, **48**, 10682.

7 (*a*) N. Cox and J. Messinger, *Biochim. Biophys. Acta, Bioenerg.*, 2013, **1827**, 1020; (*b*) A. Boussac, J.-L. Zimmermann, A. W. Rutherford and J. Lavergne, *Nature*, 1990, **347**, 303; (*c*) B. J. Hallahan, J. H. A. Nugent, J. T. Warden and M. C. W. Evans, *Biochemistry*, 1992, **31**, 4562; (*d*) A. Boussac and A. W. Rutherford, *Biochemistry*, 1992, **31**, 7441; (*e*) J. Stubbe and W. A. van der Donk, *Chem. Rev.*, 1998, **98**, 705; (*f*) M. L. Gilchrist, Jr., J. A. Ball, D. W. Randall and R. D. Britt, *Proc. Natl. Acad. Sci. U. S. A.*, 1995, **92**, 9545; (*g*) X.-S. Tang, D. W. Randall, D. A. Force, B. A. Diner and R. D. Britt, *J. Am. Chem. Soc.*, 1996, **118**, 7638.

8 T. Takashima, K. Hashimoto and R. Nakamura, *J. Am. Chem. Soc.*, 2012, **134**, 18153.

9 (*a*) T. Takashima, K. Hashimoto and R. Nakamura, *J. Am. Chem. Soc.*, 2012, **134**, 1519; (*b*) T. Takashima, A. Yamaguchi, K. Hashimoto, H. Irie and R. Nakamura, *Electrochemistry*, 2014, **82**, 325.

10 I. I. Mazin, D. I. Khomskii, R. Lengsdorf, J. A. Alonso, W. G. Marshall, R. M. Ibberson, A. Podlesnyak, M. J. Martínez-Lope and M. M. Abd-Elmeguid, *Phys. Rev. Lett.*, 2007, **98**, 176406.

11 A. Yamaguchi, R. Inuzuka, T. Takashima, T. Hayashi, K. Hashimoto and R. Nakamura, *Nat. Commun.*, 2014, **5**, 4256.

12 (*a*) M. M. Najafpour, M. Z. Ghobadi, B. Haghighi, T. Tomo, R. Carpentier, J.-R. Shen and S. I. Allakhverdiev, *Plant Physiol. Biochem.*, 2014, **81**, 3; (*b*) M. M. Najafpour, M. Z. Ghobadi, D. J. Sedigh and B. Haghighi, *RSC Adv.*, 2014, **4**, 39077; (*c*) M. M. Najafpour, D. J. Sedigh, S. M. Hosseini and I. Zaharieva, *Inorg. Chem.*, 2016, **55**, 8827.

13 (*a*) M. J. Russell and A. J. Hall, presented in part at Sixth International Congress on Carbon Dioxide Utilization, Breckenridge, Colorado, September, 2001; (*b*) K. Sauer and V. K. Yachandra, *Proc. Natl. Acad. Sci. U. S. A.*, 2002, **99**, 8631.

14 (*a*) R. M. McKenzie, *Mineral. Mag.*, 1971, **38**, 493; (*b*) M. Singh, D. N. Thanh, P. Ulbrich, N. Strnadová and F. Štěpánek, *J. Solid State Chem.*, 2010, **183**, 2979.

15 (*a*) E. Gileadi, *Electrode kinetics for chemists, chemical engineers, and materials scientists*, Wiley-VCH, New York, 1993; (*b*) J. O'M. Bockris, *J. Chem. Phys.*, 1956, **24**, 817.

16 W. P. Jencks, *J. Am. Chem. Soc.*, 1972, **94**, 4731.

17 W. M. Haynes, *CRC Handbook of Chemistry and Physics*, CRC Press, Boca Raton, 2014.

18 S. Navaratnam and B. J. Parsons, *J. Chem. Soc., Faraday Trans.*, 1998, **94**, 2577.

19 A. Harriman, *J. Phys. Chem.*, 1987, **91**, 6102.

20 M. H. V. Huynh and T. J. Meyer, *Chem. Rev.*, 2007, **107**, 5004.

21 (*a*) C. P. Kelly, C. J. Cramer and D. G. Truhlar, *J. Phys. Chem. B*, 2006, **110**, 16066; (*b*) A. A. Isse and A. Gennaro, *J. Phys. Chem. B*, 2010, **114**, 7894.

22 B. Jagoda-Cwiklik, P. Slavíček, L. Cwiklik, D. Nolting, B. Winter and P. Jungwirth, *J. Phys. Chem. A*, 2008, **112**, 3499.

23 C. Tommos, J. J. Skalicky, D. L. Pilloud, A. J. Wand and P. L. Dutton, *Biochemistry*, 1999, **38**, 9495.

24 (*a*) S. Yoshikawa and A. Shimada, *Chem. Rev.*, 2015, **115**, 1936; (*b*) S. A. Roberts, A. Weichsel, G. Grass, K. Thakali, J. T. Hazzard, G. Tollin, C. Rensing and W. R. Montfort, *Proc. Natl. Acad. Sci. U. S. A.*, 2002, **99**, 2766.